Triple Arterial Phase CT of the Liver with Radiation Dose Equivalent to That of Single Arterial Phase CT: Initial Experience

Brehmer, Katharina ; Brismar, Torkel B ; Morsbach, Fabian ; Svensson, Anders ; Stål, Per ; Tzortzakakis, Antonios ; Voulgarakis, Nikolaos ; Fischer, Michael A

Abstract: Purpose To develop and evaluate a triple arterial phase CT liver protocol with a similar radiation dose to that of standard single arterial phase CT in study subjects suspected of having hepatocellular carcinoma (HCC). Materials and Methods The study consisted of a retrospective part A for protocol development (n = 15) and a prospective part B to evaluate diagnostic accuracy (n = 38). All 53 participants underwent perfusion CT with 50 mL contrast material between August 2013 and September 2014. Group B underwent an additional standard multiphasic liver CT examination with 120 mL of contrast material (range, 70-143 mL). Image sets from triple arterial phase imaging were reconstructed from perfusion CT by fusing images from three dedicated arterial time points. Triple arterial phase CT and standard single arterial phase CT were compared by two readers, who assessed subjective image quality and HCC detection rate. A third reader served as reference reader and assessed objective image quality. The paired Student t test, Wilcoxon signed rank test, jackknife alternative free-response receiver operating characteristic (JAFROC), and JAFROC curve were applied. Results The mean volume CT dose index was 11.6 mGy for triple arterial phase CT and 11.9 mGy for standard single arterial phase CT (P = .73). Triple arterial phase CT showed lower image noise and better contrast-to-noise ratio compared with standard single arterial phase CT (P < .001 and P = .032, respectively); however, there was no significant difference in lesion-to-liver-contrast ratio (P = .31). Subjective image quality was good for both protocols. The detection rate of the 65 HCC lesions was 82% for reader 1 and 83% for reader 2 at triple arterial phase CT and 80% for reader 1 and 77% for reader 2 at standard single arterial phase CT (P = .4). Conclusion Triple arterial phase imaging is feasible at the same radiation dose as that used for standard single arterial phase CT. Triple arterial phase imaging provides equivalent to superior image quality and equal HCC detection rate despite the use of less than half the contrast material dose used at standard single arterial phase CT. © RSNA, 2018.

DOI: https://doi.org/10.1148/radiol.2018172875

DOI: https://doi.org/10.1148/radiol.2018172875

Triple Arterial Phase CT of the Liver with Radiation Dose Equivalent to That of Single Arterial Phase CT: Initial Experience

Katharina Brehmer, MD • Torkel B. Brismar, MD, PhD • Fabian Morsbach, MD, PhD • Anders Svensson, PhD • Per Stål, MD, PhD • Antonios Tzortzakakis, MD • Nikolaos Voulgarakis, MD • Michael A. Fischer, MD

From the Department of Clinical Science, Intervention and Technology (CLINTEC), Radiology Unit, Karolinska Institutet, Alfred Nobels alle 8, 141 52 Huddinge, C1:46 14186 Stockholm, Sweden. Received December 17, 2017; revision requested February 15, 2018; final revision received March 16; accepted March 29. **Address correspondence to** K.B. (e-mail: *katharina.brehmer@ki.se*).

Conflicts of interest are listed at the end of this article.

Radiology 2018; 289:111–118 • https://doi.org/10.1148/radiol.2018172875 • Content codes: CT GI

Purpose: To develop and evaluate a triple arterial phase CT liver protocol with a similar radiation dose to that of standard single arterial phase CT in study subjects suspected of having hepatocellular carcinoma (HCC).

Materials and Methods: The study consisted of a retrospective part A for protocol development (n = 15) and a prospective part B to evaluate diagnostic accuracy (n = 38). All 53 participants underwent perfusion CT with 50 mL contrast material between August 2013 and September 2014. Group B underwent an additional standard multiphasic liver CT examination with 120 mL of contrast material (range, 70–143 mL). Image sets from triple arterial phase imaging were reconstructed from perfusion CT by fusing images from three dedicated arterial time points. Triple arterial phase CT and standard single arterial phase CT were compared by two readers, who assessed subjective image quality and HCC detection rate. A third reader served as reference reader and assessed objective image quality. The paired Student t test, Wilcoxon signed rank test, jackknife alternative free-response receiver operating characteristic (JAFROC), and JAFROC curve were applied.

Results: The mean volume CT dose index was 11.6 mGy for triple arterial phase CT and 11.9 mGy for standard single arterial phase CT (P = .73). Triple arterial phase CT showed lower image noise and better contrast-to-noise ratio compared with standard single arterial phase CT ($P < .001$ and P = .032, respectively); however, there was no significant difference in lesion-to-liver-contrast ratio (P = .31). Subjective image quality was good for both protocols. The detection rate of the 65 HCC lesions was 82% for reader 1 and 83% for reader 2 at triple arterial phase CT and 80% for reader 1 and 77% for reader 2 at standard single arterial phase CT (P = .4).

Conclusion: Triple arterial phase imaging is feasible at the same radiation dose as that used for standard single arterial phase CT. Triple arterial phase imaging provides equivalent to superior image quality and equal HCC detection rate despite the use of less than half the contrast material dose used at standard single arterial phase CT.

Primary liver cancer, including hepatocellular carcinoma (HCC), is the sixth most common cancer in the world (1), with a mean 5-year survival rate of 5%–20% (2). Curative treatment for HCC can be achieved with surgical resection, liver transplantation, or radiofrequency ablation. According to the Barcelona Clinic Liver Cancer criteria, curative treatment is only advocated to asymptomatic patients with early HCC (3). Thus, as early diagnosis is crucial to enable curative treatment, improving the HCC detection rate would be directly beneficial for patient care and survival.

Currently, the diagnosis of HCC is predominantly based on cross-sectional imaging (4,5), and needle biopsy is only seldomly required. Imaging-based diagnosis of HCC relies on HCC-specific imaging features in patients with chronic liver disease, including hyperenhancement on late arterial phase images and washout at the portal venous and/or delayed phases of multiphasic contrast material–enhanced imaging. However, previous studies have shown that arterial hyperenhancement can be absent in as many as 18% of HCCs (6). Accordingly, the detection rate of HCC, especially when smaller than 2 cm, is poor at multiphasic CT and MRI (7–9), which might be due either to a weak arterial supply of early HCC or to suboptimal arterial phase timing of standard multiphasic imaging (10). Multiple arterial phase imaging with MRI (11), as well as arterial perfusion maps derived from several arterial time points of a CT perfusion study, have been shown to improve the sensitivity for detecting HCC (12), underlining the importance of accurate contrast material timing in HCC.

Acquisition of multiple arterial subphases by using CT is associated with a substantial increase in radiation dose compared with single-phase imaging. However, recent developments in postprocessing of perfusion CT with a spatiotemporal multiband (frequency dependent) filtering technique allow substantial noise reduction and fusion of images from several arterial time points into a single time-resolved maximum intensity projection (MIP) (13,14). These postprocessing steps were shown to improve image quality (15). Consequently, as each arterial time point can be acquired at very low doses, fusion of images from several arterial time points into a single time-resolved MIP might increase the detection rate of HCC compared with that at

Abbreviations

HCC = hepatocellular carcinoma, JAFROC = jackknife alternative free-response receiver operating characteristic, MIP = maximum intensity projection, ROI = region of interest

Summary

The triple arterial phase maximum intensity projection (MIP) protocol is feasible at the same radiation dose as that used with a standard single arterial phase protocol by using a new postprocessing technique. Triple arterial phase MIP provides equivalent-to-superior image quality and an equal hepatocellular carcinoma detection rate despite using less than half the contrast material dose used at standard single arterial phase CT.

Implications for Patient Care

- Fusion of low-radiation-dose images obtained at three time points improves the contrast-to-noise ratio at arterial phase imaging without increasing total radiation dose.
- The possibility of reducing contrast material dose from 120 mL to 50 mL without compromising hypervascular lesion detection sensitivity at liver imaging might be useful for patients with chronic kidney disease.
- The detection of hepatocellular carcinoma might improve if triple arterial phase imaging is integrated in a standard full contrast material dose CT protocol.

standard late arterial phase CT by combining information from several arterial phases and/or time points.

Our aim was to design a multiple arterial phase protocol with a dose equivalent to that with a standard late arterial phase protocol by means of image fusion and noise reduction of several arterial time points. Moreover, we evaluated the detection rate of HCC by comparing the newly designed multiarterial phase protocol with the standard late arterial phase protocol.

Materials and Methods

The regional ethical review board approved the study, and informed consent was obtained. The study consisted of two parts. In the first part, a dose-equivalent triple arterial phase MIP protocol was retrospectively designed from previously acquired perfusion CT data. In the second part, triple arterial phase time-resolved MIP images were prospectively simulated and compared with late arterial phase (single arterial phase) images from standard CT for evaluation.

Design of a Dose-equivalent Triple Arterial Phase Protocol

Group A.—The retrospective study group (group A) consisted of 15 subjects who underwent perfusion CT between March 2012 and August 2014. There were 13 men (87%) and two women (13%), with a mean age (±standard deviation) of 65 years ± 10 (range, 53–84 years). The subjects had liver cirrhosis due to either viral hepatitis (nine subjects, 60%) or alcoholic liver disease (six subjects, 40%). There was a total of 27 HCC lesions in the 15 subjects. Nine of the 15 subjects (60%) had Child-Pugh class A disease, five subjects (33%) had Child-Pugh class B disease, and one subject (7%) had Child-Pugh class C disease.

Arterial peak enhancement of HCC.—The average volume CT dose index (in milligrays) at a single time point of a low-dose dynamic perfusion protocol was compared with volume CT dose index values at the late arterial phase of a standard liver CT protocol with the same kilovolt setting (80 kV). The evaluation showed that the combined radiation dose of three time points of perfusion CT was equivalent to that at one standard arterial phase at the reported protocol parameters (Tables 1, 2).

Thereafter, we obtained time-attenuation curves of all 27 HCCs in group A. Peak enhancement times were determined by using commercially available postprocessing software (CT Dynamic Angio, syngo.via; Siemens Healthineers, Forchheim, Germany). The peak enhancement times were corrected for cardiac output variations by subtracting the time until 160 Hounsfield units (HU) was reached in the abdominal aorta, simulating the bolus-tracking technique for contrast material timing. Minimum, mean, and maximum values of these corrected peak enhancement times served as the reference for prospectively selecting three arterial time points for the triple arterial phase protocol (Fig 1).

Performance of the Dose-equivalent Triple Arterial Phase Protocol

Group B.—Between August 2013 and September 2014, 44 consecutive study participants (group B) known to have or with a high probability of having HCC underwent dynamic perfusion CT and clinically indicated standard multiphasic liver CT on the same day by using a second-generation dual-source CT scanner (Somatom Definition Flash, Siemens Healthineers). Exclusion criteria were as follows: age younger than 50 years, renal insufficiency (defined as serum creatinine level <1.2 mg/dL), or known iodine intolerance. Four of the 44 subjects (9%) were excluded for technical reasons, including incorrect kilovolt settings (n = 2), insufficient liver coverage (n = 1), and delayed scanning start (n = 1). Two other participants (5%) had to be excluded because they had more than 10 liver lesions. Thus, a total of 38 subjects were included.

Of the 38 participants in group B, there were 33 men (87%) and five women (13%). The mean age was 66 years ± 8 (range, 51–87 years). Thirty-two of the 38 participants (84%) had cirrhosis and two (5%) had fibrosis. Four of the 38 participants (11%) had neither cirrhosis nor fibrosis. Of the 32 participants with cirrhosis, 21 subjects (66%) had Child-Pugh class A disease, 10 subjects (31%) had Child-Pugh class B disease, and one subject (3%) had Child-Pugh class C disease. The main reasons for cirrhosis were hepatitis C virus infection (n = 12), hepatitis C virus infection combined with alcoholic liver disease (n = 8), alcoholic liver disease (n = 3), and nonalcoholic fatty liver disease (n = 2). For one study participant, the cause of cirrhosis was unknown. In the remaining six subjects, cirrhosis was caused by cryptogenic cirrhosis (n = 1), primary sclerosing cholangitis (n = 1), autoimmune hepatitis (n = 1), hepatitis B virus infection (n = 1), hepatitis B virus infection combined with hepatitis C virus infection (n = 1), and hepatitis C virus infection combined with hemochromatosis (n = 1).

Of the 53 participants from group A and B combined, 15 subjects have been previously reported on in other published studies (12,15–17). However, the current study exploits a different study aim, methodology, and results as compared with the previous publications. Whereas previous studies dealt with perfusion CT of the liver and focused on technical refinements of the perfusion CT technique (15,17), as well as on diagnostic performance of perfusion mapping for the detection of HCC (12,16), the present study evaluates the feasibility, image quality, and diagnostic accuracy of a newly developed triple arterial phase CT liver protocol.

Table 1: CT Protocols

Parameter	Perfusion CT	Standard Late Arterial Phase CT
Scanning parameter		
z-axis coverage (cm)*	19.2 (15.5–22.1)	26.0 (20.1–50.9)
Scanning delay (sec)	8	Bolus tracking +20
No. of scans*	28 (26–30)	1
Scanning direction	Craniocaudal alternating	Craniocaudal
Cycle time (sec)	1.5–1.75	…
Total acquisition time (sec)*	48 (43–54)	…
Pitch	…	0.7
Tube voltage (kV)	80	80
Tube current (mAs)	160	Automatic tube current modulation
Section collimation (mm)	128 × 0.6	128 × 0.6
Gantry rotation time (msec)	285	500
Contrast material injection protocol		
Volume (mL)	50	120 (70–143), adjusted to body weight
Iodine concentration (mg/mL)	400	400
Flow rate (mL/sec)	6	4.7 (2.9–5.6)
Injection duration (sec)	8.3	25

* Data are means, with range in parentheses.

Table 2: Mean Radiation Doses

Parameter	Perfusion CT		Standard Late Arterial Phase CT
	Single Time Point	Three Time Points (Triple Arterial Phase)	
$CTDI_{vol}$ (mGy)	3.88	11.64	11.85
DLP (mGy × cm)*	74.50	223.32	227.52
Effective dose (mSv)†	1.12	3.35	3.41

Note.—$CTDI_{vol}$ = volume CT dose index, DLP = dose-length product.

* z-axis coverage was 19.2 cm.

† Abdominal conversion coefficient = 0.015.

CT imaging and reconstruction.—The scanning and contrast material protocols for standard CT and perfusion CT are detailed in Table 1. Although both examinations were performed at 80 kV, a significantly lower amount of contrast material was used for the perfusion CT protocol (mean volume, 50 mL) than for the standard CT protocol (mean volume, 120 mL) ($P < .001$).

Triple arterial phase MIP reconstruction was performed for all 38 study subjects in group B by using the same software application as mentioned earlier. A triple-phase MIP is a time-resolved MIP that displays information from all three arterial time points in one image set. The images from the three prospectively defined time points were identified and fused after motion correction and noise-reduction postprocessing steps were applied. For noise reduction, a multiband spatiotemporal filter was used. This postprocessing technique first separates high- and low-frequency bands. For the low frequencies, which contain contrast material information and time-attenuation information, the original data are preserved. Edges and noise, on the other hand, are covered by high-frequency bands. The high frequencies are averaged to reduce pixel noise. Last, high- and low-frequency bands are recombined to create the final noise-reduced images (13,14).

Both the triple arterial phase MIP images derived from perfusion CT and the single arterial phase images derived from standard CT were presented in axial stacks with 3-mm-thick sections and an increment of 1.5 mm.

HCC detection and subjective image quality assessment.—Thirty-eight triple arterial phase MIP image sets and the corresponding 38 single arterial phase image sets were evaluated by two abdominal radiologists (reader 1 [A.T.] and reader 2 [N.V.], with 10 and 8 years of experience, respectively, in abdominal CT). The readers independently read a mix of 19 randomly ordered triple arterial phase MIP image sets and a different set of 19 single arterial phase image sets on two separate occasions. The second reading took place 4 weeks after the first reading to minimize recall bias. Readers were blinded to all clinical information and to the radiology report. Only minimal annotations were allowed in the picture archiving and communication system (version IDS7; Sectra, Linköping, Sweden). Readers did not have access to the other series of the standard multiphasic liver CT (unenhanced scan, portal venous phase and delayed phase scans). The two readers assessed one image set at a time (ie, from either triple arterial phase MIP or single arterial phase MIP) to detect hypervascular lesions larger than 9 mm in diameter with a masslike and/or round appearance.

The number of HCC lesions was defined by a reference reader (reader 3 [K.B.], with 7 years of experience in abdominal CT) with use of the complete multiphasic standard CT set (unenhanced scan and late arterial, portal venous, and delayed phase

scans) and follow-up images according to American Association for the Study of Liver Diseases/European Association for the Study of the Liver criteria (4,5) in 30 of 38 participants (79%) and/or histopathology reports in 11 (29%). The mean total follow-up time was 507 days (range, 74–897 days).

Readers 1 and 2 also assessed subjective overall image quality, arterial vessel depiction, and lesion depiction quality by using a four-point Likert scale, where 1 = poor, 2 = moderate, 3 = good, and 4 = excellent. In addition, they graded the presence and severity of motion artifacts as follows: 1 = nondiagnostic, severe artifacts; 2 = partly diagnostic, moderate artifacts; 3 = diagnostic, minimal artifacts; and 4 = diagnostic, no artifacts.

Objective image quality analysis.— Reader 3 furthermore analyzed quantitative image quality by placing circular regions of interest (ROIs). To evaluate lesion-to-liver contrast, lesion-to-liver contrast ratio, and contrast-to-noise ratio, one ROI was placed to delineate the hypervascular part of the lesion and two ROIs were placed in the liver parenchyma in close proximity to the lesion, avoiding vessels and other possible inhomogeneities (Fig 2).

Liver-to-lesion contrast was calculated by subtracting the mean CT number in the lesion from the mean CT number in the liver. The lesion-to-liver contrast ratio was calculated by dividing the liver-to-lesion contrast by the CT number in the liver. The contrast-to-noise ratio was calculated by dividing the liver-to-lesion contrast by the mean standard deviation of the attenuation measurement in the liver.

For the evaluation of image noise, two additional ROIs were placed in the air surrounding the study subject. Image noise was calculated as follows: (mean standard deviation$_{liver}$ + mean standard deviation$_{air}$)/2.

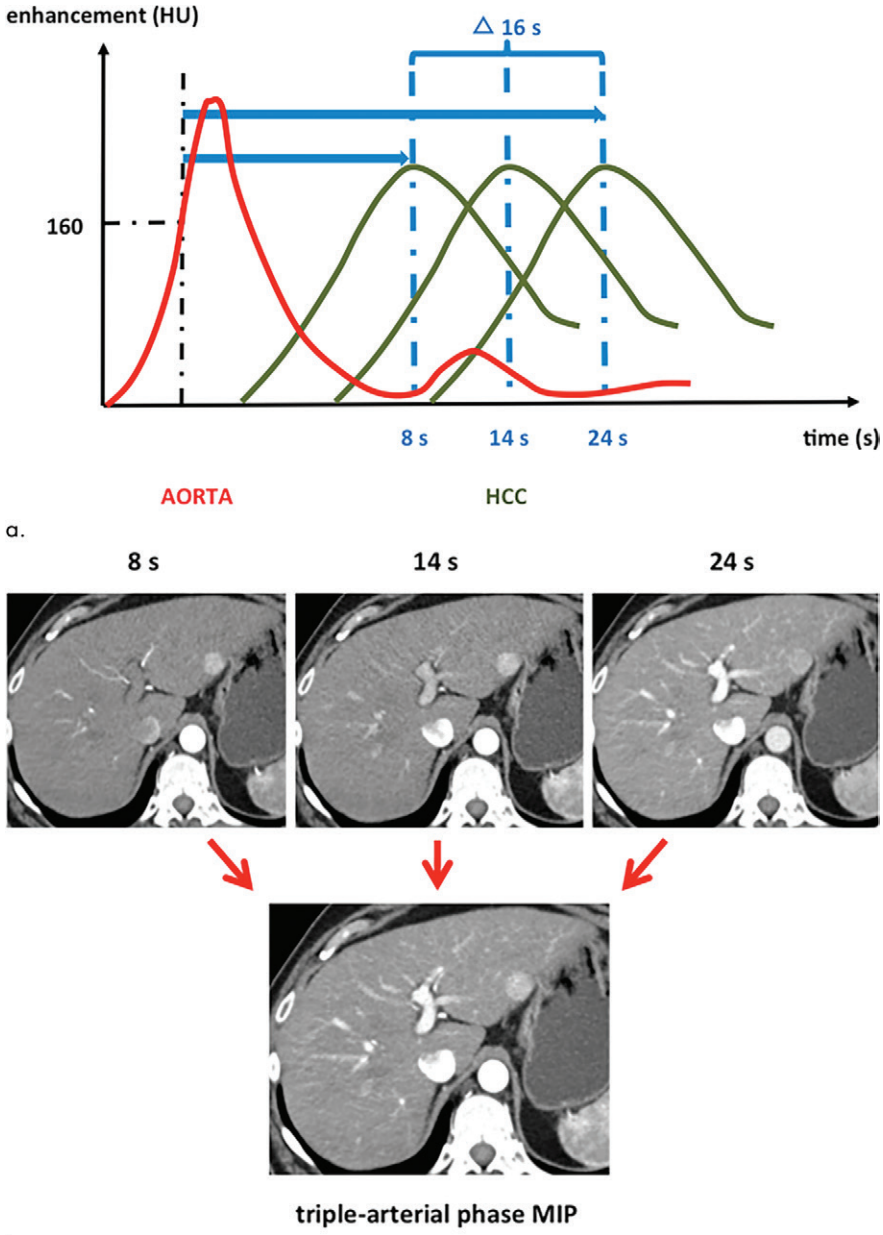

Figure 1: **(a)** Diagram illustrates variation of peak enhancement times in 27 hepatocellular carcinomas (HCCs) from 15 participants in group A. Enhancement curves for the HCCs with the minimum (8 seconds), mean (14 seconds), and maximum (24 seconds) times to peak enhancement are shown. Peak enhancement times were corrected for cardiac output variations by subtracting the time until 160 HU was reached in abdominal aorta. Red curve = aorta, green curves = HCC lesions. Black dashed vertical line indicates time point when 160 HU was reached in abdominal aorta. Blue dashed vertical lines indicate peak enhancement in each of the three shown HCC enhancement curves. **(b)** CT images in 58-year-old man with biopsy-proven HCC in liver segment III. CT images from these three specific arterial time points were isolated from a complete perfusion CT data set and fused into one time-resolved triple arterial phase maximum intensity projection (MIP) image.

Statistical Methods

Quantitative data were descriptively reviewed and tested for normality by using the Shapiro-Wilk test. Normally distributed variables were compared by using the paired Student *t* test. Nonparametric data were compared by using the Wilcoxon signed rank test. Calculated sensitivities for each reader are presented with the Wilson confidence interval. True- and false-positive ratings were determined. Confidence ratings (of the Likert Scale) were analyzed by using the jackknife alternative free-response receiver operating characteristic (JAFROC) as described by Chakraborty (18). The performance of triple arterial phase MIP and single arterial phase CT was estimated by using the area under the JAFROC curve, including 95% confidence intervals.

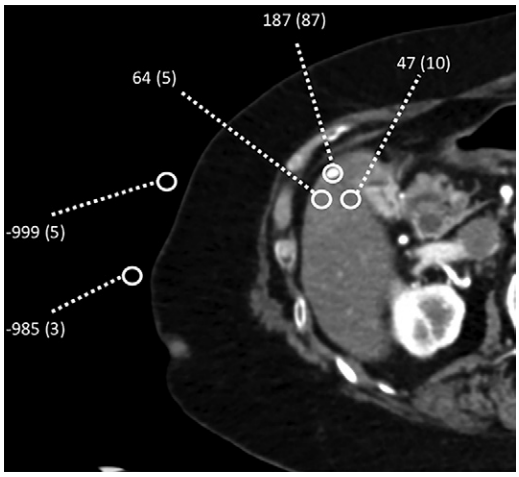

Figure 2: Example of region of interest (ROI) placement for objective image quality analysis. CT image was obtained in 56-year-old woman with arterial hyperenhancing lesion in liver segment V. One ROI delineates lesion, two ROIs are in liver parenchyma surrounding the lesion, and two ROIs are in air. All ROIs are 0.40 cm^2. Numbers indicate attenuation inside ROIs, in Hounsfield units. Numbers in parentheses are standard deviation of each measurement, which was used for noise assessment.

Table 3: HCC Detection Rates

Reader and Protocol	No. of True-Positive Findings	No. of False-Positive Findings	Sensitivity (%)
Reader 1			
Triple arterial phase protocol	53	30	82 (70, 89)
Single arterial phase protocol	52	39	80 (69, 88)
Reader 2			
Triple arterial phase protocol	54	20	83 (72, 90)
Single arterial phase protocol	50	30	77 (65, 85)

Note.—There were 65 hepatocellular carcinomas (HCCs). Numbers in parentheses are 95% confidence intervals. For overall performance, the area under the curve for the triple arterial phase protocol was 0.73 (95% confidence interval: 0.61, 0.85). The area under the curve for the single arterial phase protocol was 0.60 (95% confidence interval: 0.43, 0.77).

The reliability of qualitative image evaluation was assessed by using the two-way random intraclass correlation coefficient of both readers, whereas the interobserver agreement for HCC detection between reader 1 and reader 2 was assessed with Cohen κ analysis. According to Landis and Koch (19), a Cohen κ coefficient of less than 0 is indicative of no agreement, 0–0.20 slight agreement, 0.21–0.40 fair agreement, 0.41–0.60 moderate agreement, 0.61–0.80 substantial agreement, and 0.81–1 almost-perfect agreement.

All statistical analyses other than JAFROC analysis were performed by using commercially available software (IBM Statistical Package for the Social Sciences Statistics, release 24.0; SPSS, Chicago, Ill). $P < .05$ was considered indicative of a statistically significant difference.

Results

Dose-equivalent Triple Arterial Phase MIP Protocol

Data postprocessing consisting of noise reduction, motion correction, and image fusion from three arterial time points was feasible in all 38 participants in group B.

Radiation doses are listed in Table 2. There was no significant difference between the mean radiation dose of triple arterial phase MIPs (mean dose-length product, 223.3 mGy × cm) derived from perfusion CT and that of single arterial phases (mean dose-length product, 227.52 mGy × cm) from standard CT ($P = .73$).

Arterial Peak Enhancement of HCC

The mean corrected time to peak enhancement of the 27 HCCs in group A was 13.4 seconds ± 3.6. The time to peak enhancement was 8.1 seconds in the fastest-enhancing HCC and 23.7 seconds in the slowest-enhancing HCC. Thus, the time to peak enhancement of all 27 HCCs had a range of 15.6 seconds even though the measurements were corrected for cardiac output variations by simulating the bolus-tracking technique (Fig 1).

Diagnostic Performance in HCC Detection

Of the 38 study participants in group B, 27 subjects (71%) had HCC, one subject (3%) had both HCC and histopathologically proven intrahepatic cholangiocarcinoma, one subject (3%) had intrahepatic cholangiocarcinoma, seven subjects (18%) had only lesions that did not fulfill diagnostic criteria for HCC, and two subjects (5%) had no visible lesions at all.

Reader 3 identified 136 lesions in total. Readers 1 and 2 detected 133 of the 136 lesions (98%). Of those 133 lesions, 65 (48.9%) fulfilled diagnostic criteria for HCC.

The average HCC size at triple arterial phase MIP was 24.7 mm (range, 10–95 mm) for reader 1 and 29.4 mm (range, 10–120 mm) for reader 2. At single arterial phase CT, the average HCC size was 25.0 mm (range, 10–115 mm) for reader 1 and 30.0 mm (range, 10–150 mm) for reader 2. There was no difference in measured size between triple arterial phase MIP and single arterial phase CT for either reader ($P = .78$ and $P = .50$, respectively).

HCC detection rates are shown in Table 3. The detection rate of the 65 HCC lesions was 82% for reader 1 and 83% for reader 2 at triple arterial phase MIP and 80% for reader 1 and 77% for reader 2 at single arterial phase CT ($P = .4$). There were no significant differences in the readers' overall performance between triple arterial phase MIP and single arterial phase CT (area under the curve: 0.73 [95% confidence interval: 0.61, 0.85] vs 0.60 [95% confidence interval: 0.43, 0.77], respectively; $P = .15$). Of the HCC lesions that were missed on single arterial phase images, seven and nine were detected by reader 1 and reader 2, respectively, on triple arterial phase MIP images (Fig 3). Of the HCC lesions that were missed on triple arterial phase MIP images, six and five were

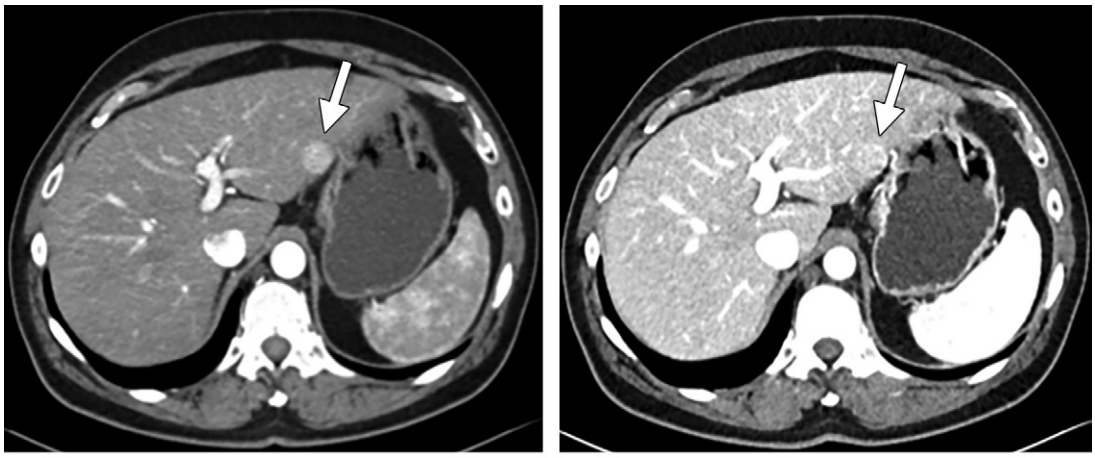

a. b.

Figure 3: CT images in 58-year-old man with histopathologically proven hepatocellular carcinoma (HCC) (arrow) in liver segment III (same subject as in Fig 1b). HCC was detected on **(a)** triple arterial phase maximum intensity projection image and missed on **(b)** standard single arterial phase image.

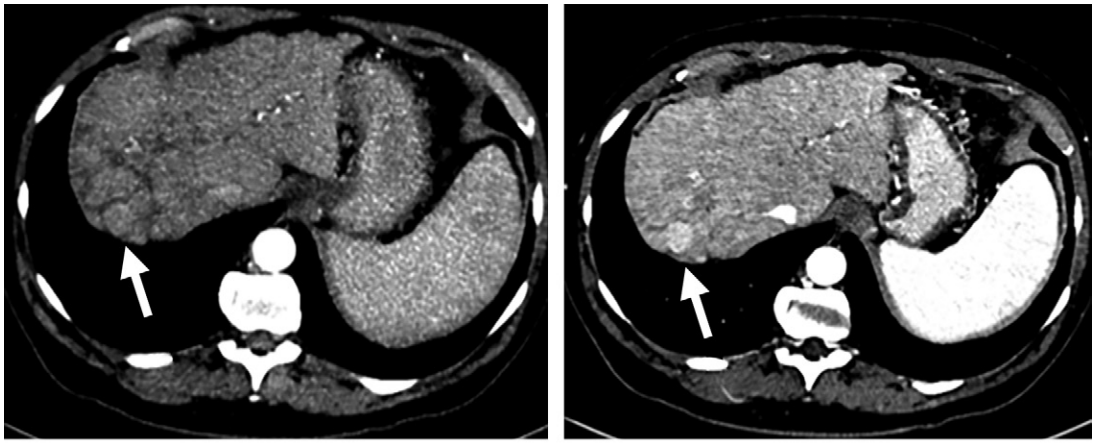

a. b.

Figure 4: CT images in 64-year-old man with a histologically proven hepatocellular carcinoma (HCC) (arrow) in liver segment VII. HCC arterial hyperenhancement was not depicted on **(a)** triple arterial phase maximum intensity projection image but was seen on **(b)** standard single arterial phase image.

detected by reader 1 and reader 2, respectively, on single arterial phase images (Fig 4). Only six of the 65 HCCs (9.2%) were missed by both readers with both protocols. Interobserver agreement was fair for both the triple arterial phase MIP image set ($\kappa = 0.366$, $P < .001$) and the single arterial phase image set ($\kappa = 0.399$, $P < .001$).

Objective and Subjective Image Quality Analysis

Results of image quality assessment are summarized in Table 4. Image noise was significantly lower ($P < .001$) and contrast-to-noise ratio significantly higher ($P = .032$) for triple arterial phase MIP image sets than for single arterial phase image sets. Lesion-to-liver contrast, however, was significantly higher for single arterial phase image sets ($P = .014$). The lesion-to-liver contrast ratio showed no significant difference between the two protocols ($P = .312$).

There was no significant difference between the protocols at subjective overall image quality assessment (reader 1: $P = .433$; reader 2: $P = .071$). The single arterial phase protocol showed significantly better results in lesion depiction quality for both readers compared with the triple arterial phase MIP protocol ($P < .001$ for readers 1 and 2). The qualitative image evaluation showed high reliability for both triple arterial phase MIP (intraclass correlation coefficient, 0.726; $P < .001$) and single arterial phase CT (intraclass correlation coefficient, 0.735; $P < .001$).

Discussion

Our study demonstrated that triple arterial phase MIP imaging with a radiation dose equivalent to that of standard single arterial phase CT is feasible. It provides an equivalent-to-superior image quality and HCC detection rate despite a lower contrast material dose than at standard late arterial phase CT.

Variations in HCC enhancement curves due to cardiac output differences were minimized by correcting peak enhancement times with use of simulated bolus tracking in the

Table 4: Image Quality

Image Quality	Triple Arterial Phase MIP	Single Arterial Phase CT	*P* Value
Objective image quality*			
Image noise (HU)	7.0 ± 2.7	15.0 ± 3.0	<.001
LLR	0.70 ± 0.59	0.75 ± 0.51	.312
LLC	51 ± 33	96 ± 54	.014
Lesion CNR	7.3 ± 6.1	4.2 ± 2.8	.032
Subjective image quality†			
Reader 1			
Arterial vessel depiction	4 (3–4)	4 (2–4)	.157
Motion artifacts	4 (4–4)	4 (3–4)	.157
Overall image quality	4 (1–4)	3 (2–4)	.433
Lesion depiction quality	2 (1–4)	3 (1–4)	<.001
Reader 2			
Arterial vessel depiction	4 (3–4)	4 (2–4)	.046
Motion artifacts	4 (2–4)	4 (3–4)	.013
Overall image quality	4 (2–4)	4 (2–4)	.071
Lesion depiction quality	3 (1–4)	4 (1–4)	<.001

Note.—CNR = contrast-to-noise ratio, HU = Hounsfield units, LLC = lesion-to-liver contrast, LLR = lesion-to-liver contrast ratio, MIP = maximum intensity projection.

* Data are means ± standard deviations.

† Data are median scores, with range in parentheses.

abdominal aorta. However, there was still a great variation in the arterial peak enhancement time of HCC, with a range of 15.6 seconds. This great variation might be due to a substantial change in arterial supply during carcinogenesis of HCC (20) and might reflect different stages of dedifferentiation. This finding is consistent with that in a previous study by Gordic et al (21) underlining the difficulty of depicting an optimally timed late arterial phase and indicating the possible benefit of capturing multiple arterial time points.

Previously, multiple arterial phase CT suffered from high radiation doses, but this limitation can now be overcome with use of noise reduction and image fusion algorithms, which markedly improve the image quality of low-dose image sets (15,22). Whereas motion correction was of minor concern in our study because the arterial phase was acquired during breath hold, the software-integrated multiband frequency–dependent filtering technique was shown to substantially reduce noise and improve image quality of the raw data (15). Interestingly, the objective image quality of reconstructed time-resolved MIPs derived from three low-dose scans was better than that of dose-equivalent standard CT images, which is in line with findings in a previous study by Wang et al (22).

Both protocols were performed with a tube voltage of 80 kV, but the standard protocol was performed with two-to-threefold higher amounts of contrast material. This resulted in stronger absolute iodine enhancement in both liver parenchyma and HCC lesions. However, although the liver-to-lesion contrast was higher with standard CT, the liver-to-lesion contrast ratio was equal for both protocols, suggesting that the relative enhancement difference in HCC versus liver parenchyma was not affected by the lower amount of contrast material used in the triple arterial phase MIP protocol. The higher amount of contrast material might also explain why subjective lesion depiction quality was superior for single arterial phase CT.

To our knowledge, this is the first study to evaluate the diagnostic performance of a triple arterial phase MIP protocol in the detection of HCC at the same radiation dose as a standard late arterial phase protocol. Our results showed that there is no overall difference in the diagnostic performance of both protocols, although the triple arterial phase MIP protocol was performed with significantly less contrast material (50 mL vs 120 mL). This may indicate that the triple arterial phase MIP protocol presented could be used in patients with renal impairment to reduce contrast material doses without losing diagnostic accuracy. We also speculate that the triple arterial phase MIP protocol with a standard iodine dose could result in higher detection rates of HCC compared with a conventional single arterial phase protocol. This concept is supported by our observation that several HCC lesions were exclusively detected on either triple arterial phase MIP images or standard single arterial phase images with a high contrast material dose. This indicates that both protocols have their benefits: better contrast material timing with triple arterial phase MIP and higher contrast material dose for the standard late arterial phase CT.

Our study had several limitations. First, the triple arterial phase MIP protocol was derived from a time-resolved perfusion CT data set consisting of 28 time points. This study showed that a dose-equivalent triple arterial phase MIP protocol is feasible, with similar to better image quality and HCC detection rates compared with standard late arterial phase imaging. However, the implementation of triple arterial phase MIP into a standard multiphasic CT liver protocol using higher contrast material doses must be further evaluated. Second, histopathologic proof of HCC was available in only 21 of the 65 HCC lesions in group B (32%); in 44 of the 65 lesions (68%), imaging follow-up served as the reference standard. Third, perfusion CT was, for logistic reasons, performed approximately 10 minutes before clinical multiphasic CT. There is a risk that residual contrast material from perfusion CT could have influenced the results of the subsequent standard single arterial phase CT examination. Moreover, the study focused on detecting arterialized lesions larger than 9 mm in chronic liver disease, which also includes entities other than HCC. However, the aim of the study was to compare the value and detection rates of the proposed triple arterial phase MIP protocol versus the standard late arterial phase protocol. Inclusion of the portal venous or late venous phases to the read-out would have influenced detection rates.

In conclusion, the triple arterial phase MIP protocol is feasible at the same radiation dose as the standard late arterial phase protocol with use of a new postprocessing technique. Triple arterial phase MIP provides equivalent-to-superior image quality and an equivalent HCC detection rate despite using less than half the contrast material dose employed at standard single arterial phase CT.

Author contributions: Guarantors of integrity of entire study, K.B., T.B.B., A.S., M.A.F.; study concepts/study design or data acquisition or data analysis/interpretation, all authors; manuscript drafting or manuscript revision for important intellectual content, all authors; approval of final version of submitted manuscript, all authors; agrees to ensure any questions related to the work are appropriately resolved, all authors; literature research, K.B., A.S., M.A.F.; clinical studies, K.B., A.S., P.S., A.T., N.V., M.A.F.; statistical analysis, K.B., F.M.; and manuscript editing, K.B., T.B.B., F.M., A.S., M.A.F.

Disclosures of Conflicts of Interest: **K.B.** disclosed no relevant relationships. **T.B.B.** disclosed no relevant relationships. **F.M.** disclosed no relevant relationships. **A.S.** disclosed no relevant relationships. **P.S.** Activities related to the present article: disclosed no relevant relationships. Activities not related to the present article: received payment for lectures including service on speakers bureaus from Bayer Sweden. Other relationships: disclosed no relevant relationships. **A.T.** disclosed no relevant relationships. **N.V.** disclosed no relevant relationships. **M.A.F.** disclosed no relevant relationships.

References

1. McGlynn KA, Petrick JL, London WT. Global epidemiology of hepatocellular carcinoma: an emphasis on demographic and regional variability. Clin Liver Dis 2015;19(2):223–238.
2. Torre LA, Bray F, Siegel RL, Ferlay J, Lortet-Tieulent J, Jemal A. Global cancer statistics, 2012. CA Cancer J Clin 2015;65(2):87–108.
3. Forner A, Reig ME, de Lope CR, Bruix J. Current strategy for staging and treatment: the BCLC update and future prospects. Semin Liver Dis 2010;30(1):61–74.
4. European Association for the Study of the Liver; European Organisation for Research and Treatment of Cancer. EASL-EORTC clinical practice guidelines: management of hepatocellular carcinoma. J Hepatol 2012;56(4):908–943.
5. Bruix J, Sherman M. Management of hepatocellular carcinoma: an update. Hepatology. 2011;53(3):1020-2.
6. Takayasu K, Arii S, Sakamoto M, et al. Clinical implication of hypovascular hepatocellular carcinoma studied in 4,474 patients with solitary tumour equal or less than 3 cm. Liver Int 2013;33(5):762–770.
7. Forner A, Vilana R, Ayuso C, et al. Diagnosis of hepatic nodules 20 mm or smaller in cirrhosis: prospective validation of the noninvasive diagnostic criteria for hepatocellular carcinoma. Hepatology 2008;47(1):97–104.
8. Lauenstein TC, Salman K, Morreira R, et al. Gadolinium-enhanced MRI for tumor surveillance before liver transplantation: center-based experience. AJR Am J Roentgenol 2007;189(3):663–670.
9. Luca A, Caruso S, Milazzo M, et al. Multidetector-row computed tomography (MDCT) for the diagnosis of hepatocellular carcinoma in cirrhotic candidates for liver transplantation: prevalence of radiological vascular patterns and histological correlation with liver explants. Eur Radiol 2010;20(4):898–907.
10. Kim KW, Lee JM, Klotz E, et al. Quantitative CT color mapping of the arterial enhancement fraction of the liver to detect hepatocellular carcinoma. Radiology 2009;250(2):425–434, s34.
11. Kazmierczak PM, Theisen D, Thierfelder KM, et al. Improved detection of hypervascular liver lesions with CAIPIRINHA-Dixon-TWIST-volume-interpolated breathhold examination. Invest Radiol 2015;50(3):153–160.
12. Fischer MA, Kartalis N, Grigoriadis A, et al. Perfusion computed tomography for detection of hepatocellular carcinoma in patients with liver cirrhosis. Eur Radiol 2015;25(11):3123–3132.
13. Liu X, Primak AN, Yu L, et al. Quantitative evaluation of noise reduction algorithms for very low dose renal CT perfusion imaging. In: Samei E, Hsieh J, eds. Proceedings of SPIE: medical imaging 2009—physics of medical imaging. Vol 7258. Bellingham, Wash: International Society for Optics and Photonics, 2009; 72581T.
14. Raupach R, Klotz E, Bruder HK, Schmidt B, Flohr TG. A new multiband spatiotemporal filter for dose reduction in 4D-CT [abstr]. In: Radiological Society of North America scientific assembly and annual meeting program. Oak Brook, Ill: Radiological Society of North America, 2009; 514.
15. Fischer MA, Leidner B, Kartalis N, et al. Time-resolved computed tomography of the liver: retrospective, multi-phase image reconstruction derived from volumetric perfusion imaging. Eur Radiol 2014;24(1):151–161.
16. Fischer MA, Marquez HP, Gordic S, et al. Arterio-portal shunts in the cirrhotic liver: perfusion computed tomography for distinction of arterialized pseudolesions from hepatocellular carcinoma. Eur Radiol 2017;27(3):1074–1080.
17. Fischer MA, Brehmer K, Svensson A, Aspelin P, Brismar TB. Renal versus splenic maximum slope based perfusion CT modelling in patients with portal-hypertension. Eur Radiol 2016;26(11):4030–4036.
18. Chakraborty DP. Analysis of location specific observer performance data: validated extensions of the jackknife free-response (JAFROC) method. Acad Radiol 2006;13(10):1187–1193.
19. Landis JR, Koch GG. The measurement of observer agreement for categorical data. Biometrics 1977;33(1):159–174.
20. Choi JY, Lee JM, Sirlin CB. CT and MR imaging diagnosis and staging of hepatocellular carcinoma. I. Development, growth, and spread: key pathologic and imaging aspects. Radiology 2014;272(3):635–654.
21. Gordic S, Puippe GD, Krauss B, et al. Correlation between dual-energy and perfusion CT in patients with hepatocellular carcinoma. Radiology 2016;280(1):78–87.
22. Wang X, Henzler T, Gawlitza J, et al. Image quality of mean temporal arterial and mean temporal portal venous phase images calculated from low dose dynamic volume perfusion CT datasets in patients with hepatocellular carcinoma and pancreatic cancer. Eur J Radiol 2016;85(11):2104–2110.